Kinetic Monte Carlo Simulations to Investigate the Effects of Interfaces in Organic Photovoltaic Cells Including a Realistic Blend Morphology

Tim Albes, Paolo Lugli, Alessio Gagliardi
Technische Universität München
Department of Electrical and Computer Engineering
Institute for Nanoelectronics
Arcisstr. 21, 80333 München, Germany
Alessio.Gagliardi@tum.de

***Abstract*—Solar cells based on organic materials are an emerging technology with a wide range of possible applications. The distribution of charge carriers in the most efficient devices, based on a bulk-heterojunction active layer structure, is hard to investigate by experiments. Modeling these cells by a kinetic Monte Carlo algorithms allows to consider a realistic morphology for the active layer and to investigate the charge densities along the interfaces between the two heterojunction materials. A major influence on the charge distribution can be attributed to the dielectric permittivity of the organic materials.**

Keywords—Monte Carlo simulations; Organic solar cells; Optimization; Permittivity;

I. INTRODUCTION

Organic photovoltaic (OPV) cells are an interesting technology with a wide development potentiality thanks to the possibility of chemically tuning the materials with ease. Moreover, the fabrication is far simpler than the one for conventional inorganic semiconductor solar cells [1-2]. State-of-the-art OPV cells are based on active layers comprised of a blend of donor and acceptor materials [3], a so called bulk-heterojunction (BHJ). The light-to-current conversion of these devices is rather complex being the interplay among many different processes and it is dominated by interfaces. Indeed interfaces are ubiquitous, especially in a bulk-heterojunction OPV cell, due to the need of efficiently splitting photogenerated excitons. The working principle of an OPV is schematically depicted in Fig. 1a).

Understanding the physical origins of the recombination of charge carriers is fundamental in achieving high performance OPVs. The exact distribution of charges inside a BHJ is among the main factors contributing to the recombination, since opposite charges are transported in different phases of the blend and can only meet and recombine at a donor acceptor interface.

The physical processes governing organic solar cells have not been totally clarified yet and the fundamental physics of device operation is still matter of investigation. Device modelling and simulation of organic solar cells is important to get an insight in the physical processes and to study the influence of different physical parameters on the efficiency of OPVs. A fundamental difference of organic materials in comparison to the most inorganic materials is their lower dielectric constant ($\varepsilon_r = 3 - 5$). The precise relationship between recombination and permittivity has not been investigated to a sufficient extent.

The standard simulation method is based on the drift-diffusion equations within the so called "effective medium" approximation [4-5], where the complexity of the morphology is approximated by a single homogeneous material with mixed properties derived from the hole and electron transport material parameters. Several important successes have been achieved using this simplification. Recently a large effort has been devoted to overcome this limitation using kinetic Monte Carlo (kMC) methods which allows to include the effective morphology in the simulation [6-8]. The main limitation in kMC

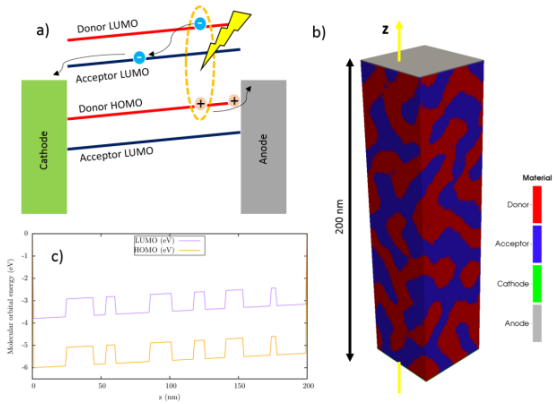

Fig. 1. (a) The fundamental operation principle of an organic solar cell: After photoexcitation a strongly Coulomb bound electron-hole pair (exciton) is formed. At a donor acceptor interface the exciton is split into electron and hole. The electrons are transported in the acceptor material and the holes are transported in the donor phase towards the contacts. (b) A spin-exchange algorithm is used to model the intermixture between donor and acceptor. (c) After system setup, the static energy distribution consists of the molecular orbital energy levels, the electric field and the energetic disorder. Lineplot along the z-axis of the structure in b)

This work was partially supported by the DFG Excellence Cluster "Nanosystems Initiative Munich" (NIM).

978-1-4673-7860-4/15/$31.00 ©2015 IEEE

simulations is the computational cost that in many cases does not permit to simulate the entire system.

We present the investigation of the charge distribution and recombination focussing on the effects of interfaces by kMC approaches within OPV, where the entire active layer is included in the simulation [9]. In particular we investigate the effect of charge accumulation at the donor acceptor interfaces throughout the BHJ.

II. MODEL

A. System Setup

To model the solar cell device the solar cell structure is discretized in an equally spaced cubic grid. The top and the bottom nodes of the grid represent the contact electrodes, while the nodes in between describe the materials of the active layer. Each node is either associated either as a donor or as an acceptor site. Before simulation starts, an algorithm to mimic the bulk-heterojunction after [10] is applied. The structure of the setup used for the simulations is shown in Fig. 1b).

The internal energy distribution for charge carriers at each node i is made up from four different contributions:

$$E_i = E_i^0 + E_i^F + E_i^D + E_i^C \qquad (3)$$

Here, the first term E_i^0 stands for the molecular orbital energy of the organic material at node i. Electrons and holes have to be treated separately by considering the LUMO or HOMO level, respectively. The electric field due to a difference in contact work functions and applied external bias is represented as a linear drop from cathode to anode across the device in E_i^F. The energetic disorder of the organic materials is chosen randomly from a Gaussian distribution with disorder parameter σ as the standard deviation. The first three terms in (3) are a static potential landscape and are fixed in a single simulation. During runtime only the Coulomb interaction term E_i^C is updated. It implemented after Casalegno [11] and includes the interaction between all charges inside the photoactive layer, across the periodic boundaries in x- and y-direction and mirror charge effects in the electrodes. Since the focus is on interface effects due to Coulomb interaction this extensive model is chosen.

B. Kinetic Monte Carlo Method

The basic structure of our model is adapted from Casalegno [11] because the treatment of Coulomb interaction ought to be as accurate as possible if one wants to study dielectric effects. The underlying kMC algorithm was developed by Gillespie [12]. Our model is described in more detail in [9] and it shall only be briefly reviewed here. After identifying the most important processes in an OPV, the evolution of the system in time is described by a set of rate equations for all processes. The rates will change in time due to different system configurations. A process to execute next is chosen by generating a random number and comparing the number to the magnitude of all the rates that are activated. Each event has a time step assigned, also determined by a random number, to set up a trajectory of system states in time. The model is able to simulate full dynamics of excitons, electrons and holes. The set of rates considered are:

- exciton generation, diffusion, decay, and separation
- Charge hopping (transport), recombination, collection at the contacts, and injection from the contacts

The exciton generation is obtained from transfer matrix calculations [13] and considers typical reflection and interference effects in thin, organic layers in between metallic contacts. The total illumination strength is hereby fixed to $100\ mW\ cm^{-2}$. Excitons diffuse randomly as neutral particles after a random walk model, and are either separated at an interface or decay before the can reach one.

Charge transport of both electrons and holes is described by hopping between localized states (nodes) and calculated by the Miller-Abrahams formula [14]

$$a_{ij} = a_0 e^{-2\gamma\Delta r} \begin{cases} e^{-(E_j - E_i)/k_B T}, & E_j - E_i > 0 \\ 1, & E_j - E_i \leq 0 \end{cases} \qquad (2)$$

Where a_0 is a typical phonon-interaction frequency, $\gamma = 2$ is a localization constant, $\Delta r = 1\ nm$ the distance between two nearest neighbors, $E_{i,j}$ the energy at nodes i and j after Equation (1), and $k_B T = 25\ meV$ the thermal energy at room temperature. Due to the Coulomb interaction oppositely charges particles attract each other. However, since electrons are transported in the acceptor phase and holes in the donor phase, they can only meet at an interface. If two opposite charges reside at adjacent nodes, they can recombine with a recombination rate. This rate is taken from [15] and set to be $a_{ehr} = 5 \cdot 10^5 s^{-1}$. If charges are at nodes next to either the cathode or the anode, they can be collected. On the other hand, charge injection from the contacts can take place where the electrodes are considered as charge reservoirs. Both injection and collection is also modeled by the Miller-Abrahams formula but with a fixed energy level for the contact work function. A list of all simulation parameters used is shown in Table 1.

TABLE I. SIMULATION PARAMETERS

Parameter	Values
Size x direction	50 nm
Size y direction	50 nm
Size z direction	200 nm
Lattice constant	1 nm
Relative permittivity	3 to 5
Work function cathode	4.3 eV
Work function anode	4.95 eV
Acceptor HOMO level	6.0 eV
Acceptor LUMO level	3.8 eV
Donor HOMO level	5.17 eV
Donor LUMO level	3.0 eV
Average cluster size	15.7 nm
Simulated time	10 nm

C. Evaluation of Charge Densities

Charge densities are evaluated by calculating the average occupancy of each node with electrons and holes, respectively. Hereby, the occupancy is weighted by the time a particle

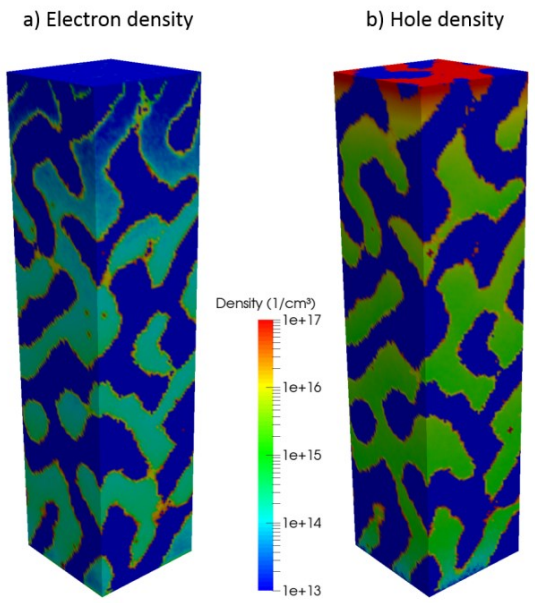

Fig. 2. Full charge density profile of the 3D active layer structure. It can clearly be seen that electrons are only located in the acceptor phase while holes reside in the donor materials. Increased hole density near the top electrode (anode) can be observed due to a lower injection barrier for

resided on a specific node and averaged over the total simulation time T.

$$< d_{ijk} >_{e^-/h^+} = \frac{10^{21}}{V_{bhj}} \frac{1}{T} \cdot \sum_{s=1}^{N} X_{ijk}^{s} \cdot \tau_s \qquad (3)$$

The volume of the total cell is V_{bhj}, and 10^{21} is a prefactor to obtain the densities in units of cm^{-3}. In each simulation time step s, where τ_s is the length of that time step, the occupancy X_{ijk} of node ijk is checked and is either 1 or 0.

III. Results and Discussion

The solar cell is simulated for a time period of $t_{sim} = 10\ ms$ to make sure steady state conditions are reached. To show the influence of the dielectric constant on the internal charge distributions, three different values for ε_r are modeled and the results compared.

To get a first insight into the internal charge distribution Fig. 2 shows the electron and hole densities evaluated throughout the total simulation time under short-circuit condition for a dielectric constant of $\varepsilon_r = 3.5$. Large deviations in the density can be observed. For one, electrons are restricted to the acceptor phase (left) with and holes are restricted to the donor phase (right). Second, an increased hole density and a depletion of electrons can be seen near the top contact, the anode. This is due to a low injection barrier for holes from the anode into the donor material. The behavior is inverted at the bottom contact (cathode) although not as pronounced. The large injection of holes at the anode and electrons at the cathode is necessary to obtain a dark current. At last and most importantly, an

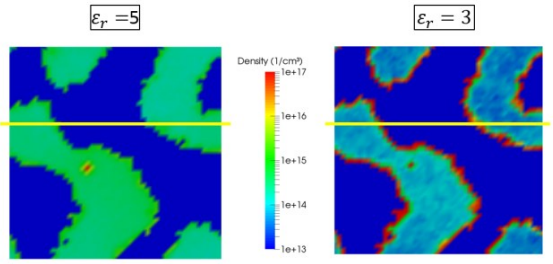

Fig. 3. Slice through the active layer at $z = 128\ nm$. The electron density is shown for two values of the dielectric constant: $\varepsilon_r = 5$ (left) and ε_r=3 (right). The accumulation of electrons at the interface for $\varepsilon_r = 3$ is pronounced.

accumulation of both electrons and holes at the donor acceptor interfaces can be observed throughout the entire active layer.

To take a closer look at the interfaces, Fig. 3 shows a slice through the active layer morphology at $z = 128\ nm$ for two different values of the dielectric constant, $\varepsilon_r = 5$ and $\varepsilon_r = 3$. Only the electron densities are shown here, but the same behavior can be seen for the holes. The accumulation of charges at the interface for the low dielectric constant is very pronounced. Indicated by a line through the slice is a lineplot along $y = 30\ nm$. Fig. 4 shows the densities along this line. Again, the variation between a dielectric constant of $\varepsilon_r = 5$ and $\varepsilon_r = 3$ clearly shows the influence on the position of charges.

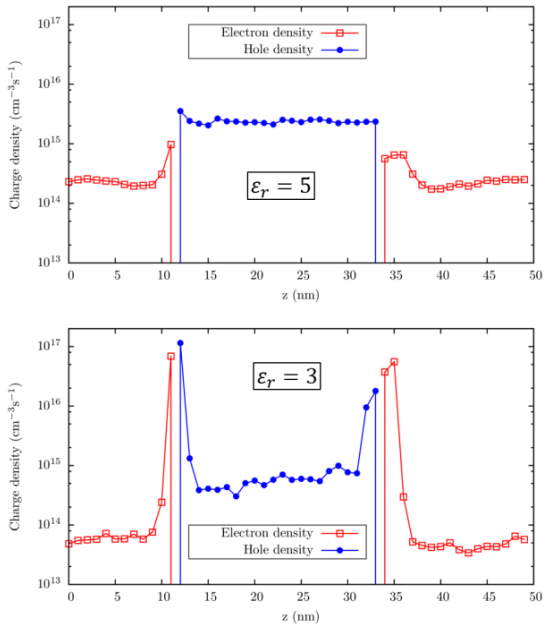

Fig. 4. Charge accumulation at the interfaces for two different values of the dielectric constant: $\varepsilon_r = 5$ (top) and $\varepsilon_r = 3$ (bottom). The charge density is given along the lineplot indicated in Fig. 4. For low dielectric constants the charge density near the interface is increased by orders of magnitude. This leads to increased recombination.

For a low dielectric constant the Coulomb forces are not well screened and act on larger distances. Opposite charges accumulate and become pulled together from inside the bulk regions towards the interfaces. While for larger dielectric constant the charge distribution is more or less uniform throughout the bulk phase and only slight accumulation can be observed. The interface charge density is up to a factor 100 higher for low permittivity than for high permittivity. This explains the dramatic effect on charge recombination: Since charges are much more likely to be found near each other more recombination takes place and the short-circuit current and fill factor are lowered as a consequence.

Quantifying this behavior, Table II indicates the ratio of recombined charges carriers with respect to the total number of charges generated by the illumination. For $\varepsilon_r = 5$ only 4.26% of all exciton generated charges recombine, while for $\varepsilon_r = 5$ the ratio dramatically increases to 65.93% for $\varepsilon_r = 3$.

TABLE II. RECOMBINATION VS. DIELECTRIC CONSTANT

Dielectric constant ε_r	Recombination R (%)
3	65.93
3.5	25.43
5	4.26

IV. CONCLUSION

Charge densities of electrons and holes in a BHJ OPV were investigated by kMC simulations with an extensive treatment of the Coulomb interactions. Charge density is found to be non-uniform and strongly dependent on the active layer geometry and the dielectric constant. Even slight modifications of the permittivity result in a major change of where charges are located. For low permittivity, Coulomb forces are not well screened and act on longer distances. This allows charges to become pulled together at the donor acceptor interface and increases recombination and therefore decreases devices performance. KMC simulations turn out to be a suitable tool to investigate the internal effects in OPV cells and to accompany the design of novel, high performance devices.

REFERENCES

[1] Søndergaard, Roar, Markus Hösel, Dechan Angmo, Thue T. Larsen-Olsen, and Frederik C. Krebs. "Roll-to-roll fabrication of polymer solar cells.*Materials today* 15, no. 1 (2012): 36-49.

[2] Kang, Jae-Wook, Yong-Jin Kang, Sunghoon Jung, Myungkwan Song, Do-Geun Kim, Chang Su Kim, and Soo H. Kim. "Fully spray-coated inverted organic solar cells.*Solar Energy Materials and Solar Cells* 103 (2012): 76-79.

[3] Sariciftci, NS; Smilowitz, L; Heeger, Alan J; Wudl, F; ,Photoinduced electron transfer from a conducting polymer to buckminsterfullerene, *Science*,258,5087,1474-1476,1992

[4] Fallahpour, A.H., et al., J. Applied Physics, **116** 184502 (2014).

[5] Fallahpour, A.H. et al., Journal of Computational Electronics **13**, p. 1-10 (2014).

[6] Giazitzidis, Paraskevas, Panos Argyrakis, Juan Bisquert, and Vyacheslav S. Vikhrenko. "Charge separation in organic photovoltaic cells." *Organic Electronics* 15, no. 5 (2014): 1043-1049.

[7] Groves, Chris, James C. Blakesley, and Neil C. Greenham. "Effect of charge trapping on geminate recombination and polymer solar cell performance." *Nano letters* 10, no. 3 (2010): 1063-1069.

[8] Kimber, Robin GE, Edward N. Wright, Simon EJ O'Kane, Alison B. Walker, and James C. Blakesley. "Mesoscopic kinetic Monte Carlo modeling of organic photovoltaic device characteristics." *Physical Review B* 86, no. 23 (2012): 235206.

[9] Albes, Tim, Bogdan Popescu, Dan Popescu, Marius Loch, Francesco Arca, and Paolo Lugli. "Kinetic Monte Carlo modeling of low-bandgap polymer solar cells." In *Photovoltaic Specialist Conference (PVSC), 2014 IEEE 40th*, pp. 0057-0062. IEEE, 2014.

[10] Watkins, Peter K., Alison B. Walker, and Geraldine LB Verschoor. "Dynamical Monte Carlo modelling of organic solar cells: The dependence of internal quantum efficiency on morphology." *Nano letters* 5, no. 9 (2005): 1814-1818.

[11] Casalegno, Mosè, Guido Raos, and Riccardo Po. "Methodological assessment of kinetic Monte Carlo simulations of organic photovoltaic devices: The treatment of electrostatic interactions." *The Journal of chemical physics* 132, no. 9 (2010): 094705.

[12] Gillespie, Daniel T. "A general method for numerically simulating the stochastic time evolution of coupled chemical reactions." *Journal of computational physics* 22, no. 4 (1976): 403-434.

[13] Burkhard, George F., Eric T. Hoke, and Michael D. McGehee. "Accounting for interference, scattering, and electrode absorption to make accurate internal quantum efficiency measurements in organic and other thin solar cells." *Advanced Materials* 22, no. 30 (2010): 3293-3297.

[14] Miller, Allen, and Elihu Abrahams. "Impurity conduction at low concentrations." *Physical Review* 120.3 (1960): 745.

[15] Marsh, R. A., C. Groves, and N. C. Greenham. "A microscopic model for the behavior of nanostructured organic photovoltaic devices."*Journal of applied physics* 101, no. 8 (2007): 083509.